ADVANCED MATERIALS
www.advmat.de

Piezo-Phototronic Effect of CdSe Nanowires

*Lin Dong, Simiao Niu, Caofeng Pan, Ruomeng Yu, Yan Zhang, and Zhong Lin Wang**

Cadmium selenide is an important II-VI semiconductor due to its distinct nonlinear optical properties, luminescent properties, quantum-size effect and the band gap in visible light range. Using these attractive properties, practical applications such as thin-film transistors,[1] light-emitting diodes,[2] photovoltaic cells,[3] optical memories,[4] sensors[5] and biomedical imaging[6] have been demonstrated. CdSe nanowires (NWs) have attracted a lot of research interest due to its unique opto-electrical properties resulting from a high aspect ratio and surface/volume ratio.[3] As a wurtzite structure crystal with non-central symmetry, a piezoelectric potential (*piezopotential*) is created in CdSe by applying a stress due to the polarization of ions. This piezopotential created in CdSe has a strong effect on the carrier transport at the interface/junction owing to the simultaneous possession of piezoelectricity and semiconductor properties, which is the origin of piezotronic and piezo-phototronic effects. The piezo-phototronic effect uses the piezopotential to control the carrier generation, transport, separation and/or recombination for improving the performance of optoelectronic devices, such as photodetectors,[7] photocells,[8] solar cells[9] and LEDs.[10,11] Most recently, several piezo-phototronic effect based thin-film devices were reported, which expand the potential application areas of piezo-phototronics from nanowire to thin-film structure.[12] ZnO and GaN have been the main materials for studying nanogenerators (NG),[13] hybrid NG,[14] piezoelectric field effect transistors (FET),[10,15] piezoelectric diodes,[16] and piezo-phototronic devices.[17] However, the piezo-phototronic effect of CdSe NWs has not been reported. In this paper, the piezo-phototronic effect on the transport behavior of CdSe NWs is demonstrated for the first time. The piezo-phototronic effect is thought to be a coupling effect due to the photo excitation, piezoelectricity and semiconductor properties of CdSe NW. The photo excitation reduces the Schottky barrier height (SBH) between CdSe and metal, while a proper applied strain can increase the SBH. The equilibrium current is determined by the coupled effects of both irradiation and applied strain. This work may offer an innovative concept to control/tune the performance of photo-sensitive flexible opto-electronic devices, such as dual-modal strain and photo imaging devices.

CdSe NWs were grown by the Au-catalyzed vapor-liquid-solid method at 800 °C and 255 Torr for 3 h, with CdSe powder as source placed at the center of the tube furnace, and a silicon wafer with 2 nm Au layer placed at 25 cm from the source at the downstream. **Figure 1**(a) shows a scanning electron microscopy (SEM) image of the CdSe NWs, showing diameters of around 0.5 μm and lengths of several hundred of micrometers. An enlarged image of a single CdSe NW is shown in Figure 1(b), clearly presenting the facets of the as-synthesized CdSe NW and the catalyst particle. The XRD pattern in Figure 1(c) indicates that the as-synthesized CdSe NWs have a wurtzite structure (PCPDF 01-077-2307). Transmission electron microscopy (TEM) image and the corresponding select area electron diffraction (SAD) pattern of a CdSe NW are presented in Figure 1(d), and the high resolution electron microscopy (HRTEM) image is given in Figure 1(e), indicating that the CdSe NWs are grown as single crystal with a growth direction along *c*-axis.

A long CdSe NW was chosen and transferred onto a flexible PET substrate (DuraLar, 1 cm × 3 cm, 500 μm in thickness) with the axis of the NW paralleling to the longitude axis of the substrate. Subsequently, both ends of the CdSe NW were fixed with silver paste, which also served as electrodes for connecting the device with external circuit. Finally, the devices were packaged with a transparent thin layer of polydimethylsiloxane (PDMS) to enhance the stability and reliability of the device. A typical optical image of the as-fabricated CdSe NW opto-device is presented in the inset of **Figure 2**(a). A schematic of the measurement setup is sketched in Figure 2(a). Both ends of the device were fixed on two sample holders tightly mounted on the micro positioning stages with a displacement resolution of 1 μm. The compressive strain was introduced by screwing in the micro positioning stages to bend the device downwards. *I–t* characteristics of the devices under different light irradiation intensities and strains were collected by a computer-controlled measurement system. To maintain a constant intensity of light illumination under different strains, the micro positioning stages were screwed in equally and the applied strain was lower than 1.0% to minimize the impacts of device deformation and obliquity on irradiation intensity.

The light-dependent current response of the CdSe NW opto-electronic device without strain is presented in Figure 2(b). The current of the device was 0.0124 nA in dark and 1.17 nA under a light illumination of 0.04 mW/cm^2, an increase by two orders of magnitude. The device has the response and relaxation time ($\tau_{1/2(\text{photo})}$) of about 38 ms. The current of the device and the light illumination intensity have a very good linear relationship in the double logarithmic chart, and the current increased to

Dr. L. Dong,[†] S. M. Niu,[†] Dr. C. F. Pan, Ruomeng Yu, Dr. Y. Zhang, Prof. Z. L. Wang
School of Materials Science and Engineering
Georgia Institute of Technology
Atlanta, GA 30332-0245, USA
E-mail: zhong.wang@mse.gatech.edu
Dr. L. Dong
School of Materials Science and Enginnering
Zhengzhou University
Zhengzhou, 450001, China
Prof. Z. L. Wang
Beijing Institute of Nanoenergy and Nanosystems
Chinese Academy of Sciences, Beijing, China
[†] These authors contributed equally to this work.

DOI: 10.1002/adma.201201385

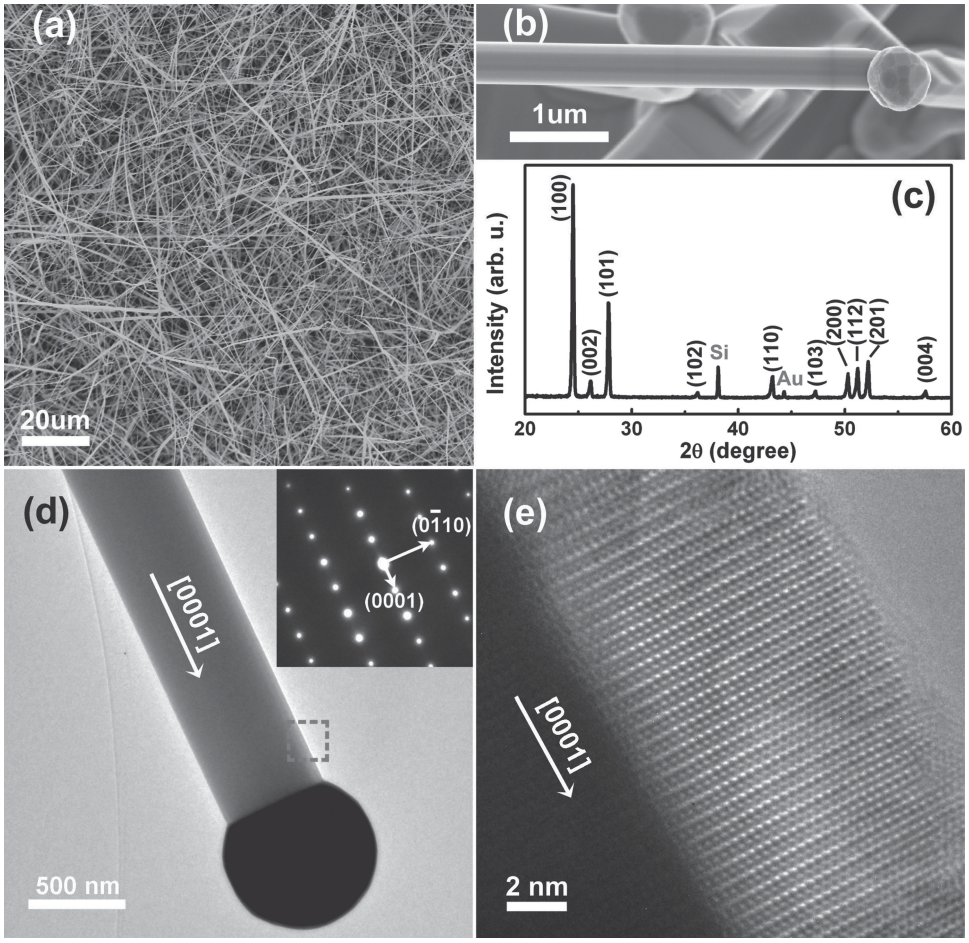

Figure 1. (a) SEM image of CdSe NWs. (b) high magnification SEM image of a CdSe NW with a catalyst particle on the tip. (c) XRD patterns of the as-grown CdSe NWs on the silicon wafer. (d) TEM image of a CdSe NW. The inset is the SAD pattern. (e) HRTEM image of the corresponding area in (d), indicating that the CdSe NW is single crystal and grown along c-axis.

16.8 nA with the illumination intensity increased to 1.26 mW/cm^2, as shown in the inset of Figure 2(b).

The strain effect on the carrier transport properties of the CdSe NW devices was carried out and the results are shown in Figure 2(c). *I–t* characteristics of the devices subjected to different strains were recorded under fixed illumination intensity of 0.20 mW/cm^2. The applied reverse bias voltage was 2 V and the applied strain rate was 0.15%$\cdot$s^{-1}, the compressive strains were applied and released for 4 cycles to validate the stability of the device. The current of the CdSe NW device was about 3.5 nA at no strain, and dropped to 3.3, 3.0, 2.8 and 2.6 nA when the applied compressive strain increased step by step from –0.53%, –0.75%, -0.92% to –1.06%, respectively; it recovered to 3.5 nA when the applied strain was released from –1.06%, –0.92%, –0.75% to –0.53% step by step, as shown in Figure 2(c). A response and relaxation time ($\tau_{1/2(\text{strain})}$) of 90 ms was obtained according to the insert plot, which is mostly due to the slow period of time for applying/retracting mechanical force. The high sensitivity on both light illumination and strain makes the CdSe NW device a promising candidate for photo detection, strain sensing and photovoltaic devices. To demonstrate the stability and reproducibility of the device, the measurement of the same device was repeated several times and the current data are consistent with each other under the same strain, which was extracted and plotted in Figure 2(d).

Then, to investigate the piezo-phototronics effect of the CdSe NW devices, a coupling effect of photo excitation and piezoelectricity, we measured the strain-dependent carrier transport properties of the CdSe NW device when the illumination intensities were fixed. A representative result obtained under an illumination intensity of 0.20 mW/cm^2 is given in **Figure 3**(a), clearly showing the trend of strain effects on equilibrium current. The equilibrium current increased from 4.41 nA to 4.94 nA as compressive strain applied on the device increased from 0% to –0.33%; and then decreased to 4.39 nA as the strain continually increased to –0.44%. Similarly as for the ZnO NWs and GaN nanobelt devices reported previously, tensile strain has an opposite effect on the transportation properties of CdSe device as compared to the compressive strain, as obtained in our experiments. However, the CdSe is much more brittle than ZnO NWs and GaN nanobelts; we cannot obtain perfectible and systematic data on this, so only piezo-phototronics effects in the compressive strain region are presented here.

Adv. Mater. **2012**,
DOI: 10.1002/adma.201201385

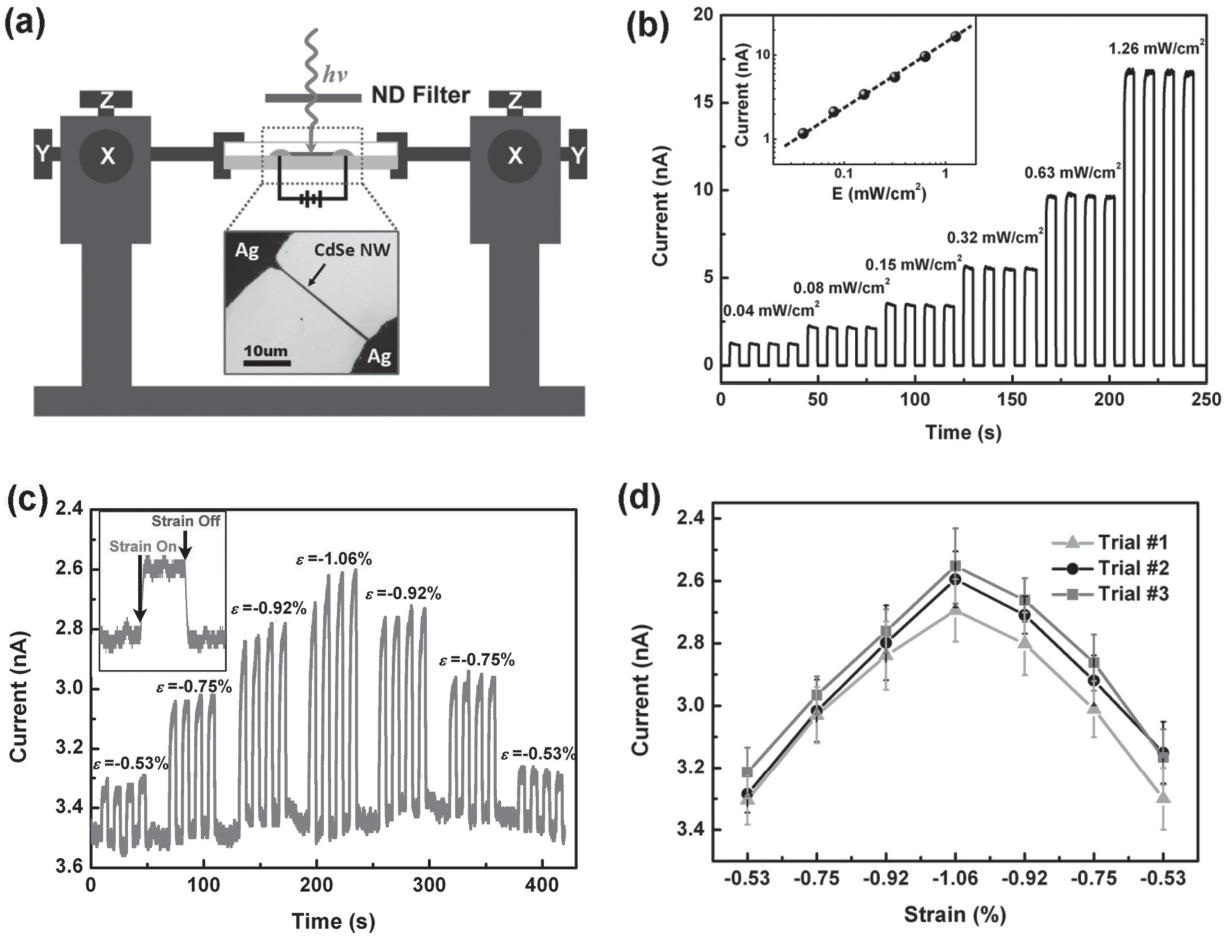

Figure 2. (a) Schematic of the measurement set-ups for studying the piezo-phototronic effect in CdSe NW, the inset is an optical image of a typical CdSe NW device. (b) Plots of the photocurrent responses of a CdSe NW device without strain under different illumination intensity. The illumination intensity increased step by step from 0.04 mW/cm^2 to 0.08, 0.15, 0.32, 0.63 and 1.26 mW/cm^2. The inset shows the double-exponential fitting result of the equilibrium current vs. illumination intensity. (c) Photocurrent response of a CdSe NW device under different compressive strains under the illumination intensity of 0.2 mW/cm2. The compressive strain applied on the device increased step by step from –0.53% to –0.75%, –0.92% and -1.06%, and then reduced to -0.53%. The inset shows a enlarged on-off response of strain. (d) Plots of the average photocurrent vs. strain under the illumination intensity of 0.2 mW/cm^2. The data was extracted from the strain response experiment shown in (c) on the same device, indicating a good reliability of the CdSe NW device.

To quantitatively study the strain effect on the transport properties of the CdSe NW opto-electronic device, here we define a strain sensitivity S, which is the relative change of the current in the devices under fixed illumination intensity, as following,

$$S = \frac{(I_s - I_0)}{I_0 \times 100\%},$$

where I_s and I_0 are the equilibrium current of the CdSe NW device with and without strain. The S at each illumination intensity is plotted to demonstrate the piezo-phototronic effect, as shown in Figure 3(b–e). When the illumination intensity is low, as shown in Figure 3(b), the photo-excited electron-hole pairs in the junction are nearly completely separated by the build-in electric field, S decreases when the compressive applied strain increases, which is in accordance with our previous theoretical work and experimental data on the piezo-phototronic controlled/tuned photo-excited carriers transport.[9,18] As for those under high illuminations intensities, when the separation of photo-excited electron-hole pairs is incomplete, all of the S curves exhibit the similar vault-like profile, i.e., they increase firstly to a maximum value when the applied strain is low, and then decrease gradually when the applied strain keeps increasing to the range marked in light blue in the Figure. The applied strain corresponding to the maximum S shifted to higher value when the illumination intensity increased. For example, the maximum S appears at a compressive strain of –0.26% under an illumination intensity of 0.049 mW/cm^2, and it occurs at a larger strain of –0.37% under a higher illumination intensity of 4.3 mW/cm^2.

The possible explanation of the results presented in Figure 2 and 3 can be interpreted by the coupling mechanism of photo-excitation and piezoelectric effect on the transport behavior of photo-excited electrons and holes. As well known, a Schottky barrier (Φ_B) is created at the interface between CdSe and Ag since the work function of the metal is appreciably larger than the electron affinity of the semiconductor, as shown in **Figure 4**(a).

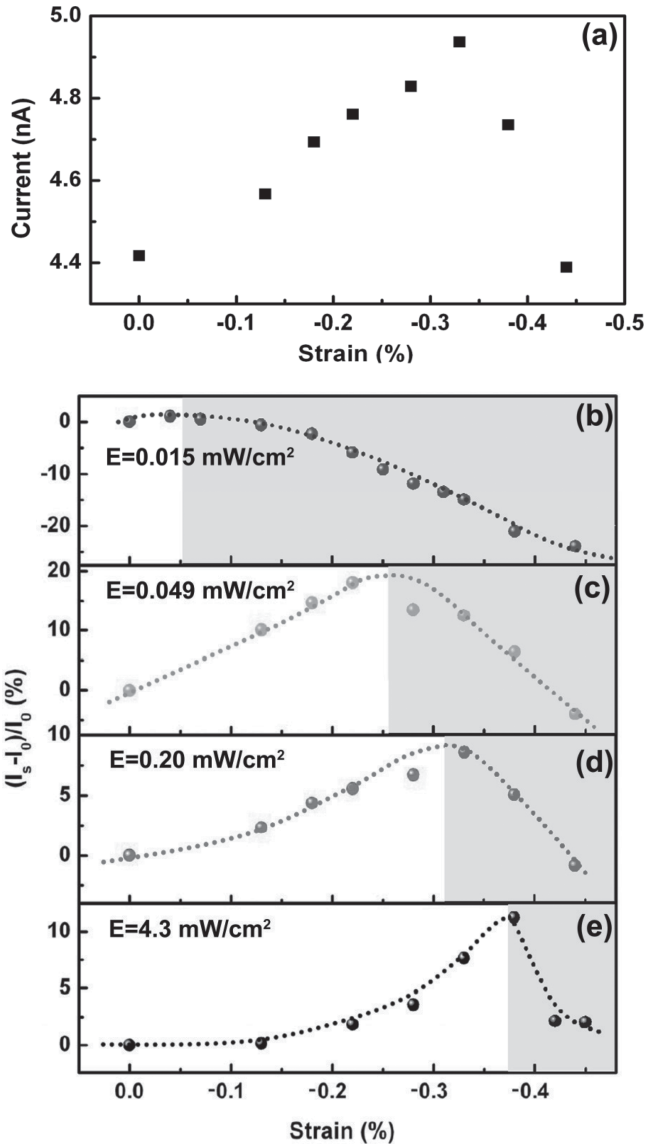

Figure 3. (a) Photocurrent of CdSe NW device under different applied strain under illumination intensity of 0.2 mW/cm^2. The applied strain was increased step by step from 0% to −0.44%. (b-e) Relative changes of the photocurrent vs. the applied strain under illumination intensity of 0.015, 0.049, 0.20 and 4.3 mW/cm^2, respectively.

For the reversely biased n-type Schottky contact without illumination, the current is determined by the SBH according to the thermionic field emission (TFE) theory.[19] When the device is under illumination as shown in Figure 4(b), the incident photons with energy higher than the bandgap of CdSe will excite electron-hole pairs; then the generated photo current depends on the effective separation and redistribution of both holes and electrons at the vicinity of the contact. As driven by the electric field of the internal Schottky junction, the photo-exited electrons in the conduction band tend to move away from the contact, while the holes tend to move close to the interface toward the metal side. The holes distributed at vicinity of the M–S junction modify the local potential profile, resulting in an obvious decrease in SBH. The stronger the incident light intensity is, the more the SBH is lowered. In this experiment, the value of the total current under illumination (I), consist of reverse biased Schottky barrier current (I_{RSB}) and photo-induced current (I_P):[18] I_{RSB}, which is driven by the reversely biased external potential, depends on the SBH; while I_P, which stems from the separation and transport of photo-excited electron-hole pairs, relies on the illumination intensity and build-in field.

When the illumination intensity is low enough, the separation of photo-excited electron-hole pairs is nearly complete and I_P can be assumed as a constant. The change in total current I is dominated by the change of I_{RSB}, which decreases with the increase of SBH due to piezotronic effect under compressive strain.[9,18] Therefore, S decreases when the compressive applied strain increases under low illumination intensity.

When the illumination intensity increases, the built-in electric field decreases dramatically as a result of the further decrease in SBH by intensive irradiation. The recombination rate of photo-excited carriers also increases due to a larger amount of excessive carriers. Hence the separation of photo-excited electron-hole pairs cannot be assumed completely. As the compressive strain is applied on the device under a fixed illumination, the negative piezoelectric charges arising from ions are generated at the M–S contact. As a non-centrosymmetric wurtzite semiconductor, the piezo-charges are originated from CdSe NW inner crystal polarization ions under strain, which are as fixed charges at the end of CdSe NW. Therefore, the electric field induced by the piezopotential at CdSe side is in the same direction as the internal electric field of the Schottky junction, which will increase the local electric field intensity in the depletion region, as shown in Figure 4(c). Considering both the photo-excited electron and hole current, the increased local electric field intensity will assist the separation of electron-hole pairs by accelerating the drifting of electrons toward the CdSe side so as to increase the photocurrent. Therefore, the total current increases when a small compressive strain was applied, as shown in the first half part of Figure 3 (c–e).

When the applied strain is high enough, the edge of the CdSe valence band at the interface is raised higher than the Fermi level of the metal. In this case, a new barrier is generated for the photo-excited holes to be transported from CdSe to the metal. The holes would be trapped at the interface, hindering the separation of photo-excited electron-hole pairs and assist the recombination of the electrons and holes at the interface of the junction,[19] subsequently resulting in a decrease in the photocurrent, as shown in the latter half part of Figure 3(c–e). That is to say, the S reaches its maximum when the positive contribution from the inner crystal field induced by piezoelectricity is balanced by the negative contribution from the interface trapping effect for the photo-excited holes. In such a case, the sensitivity of the opto-device is the highest. A further increase in strain results in lower separability of holes, thus, the measured current drops,

When the illumination intensity increases, the local SBH is further reduced, resulting in a larger deviation between the valence band edge of the CdSe and the Fermi level of the metal, which is not favorable for the separation of electrons generated at the interface. Thus, to re-achieve the optimum sensitivity of the opto-device, a larger piezo-electric field is required to lift up

Adv. Mater. 2012,
DOI: 10.1002/adma.201201385

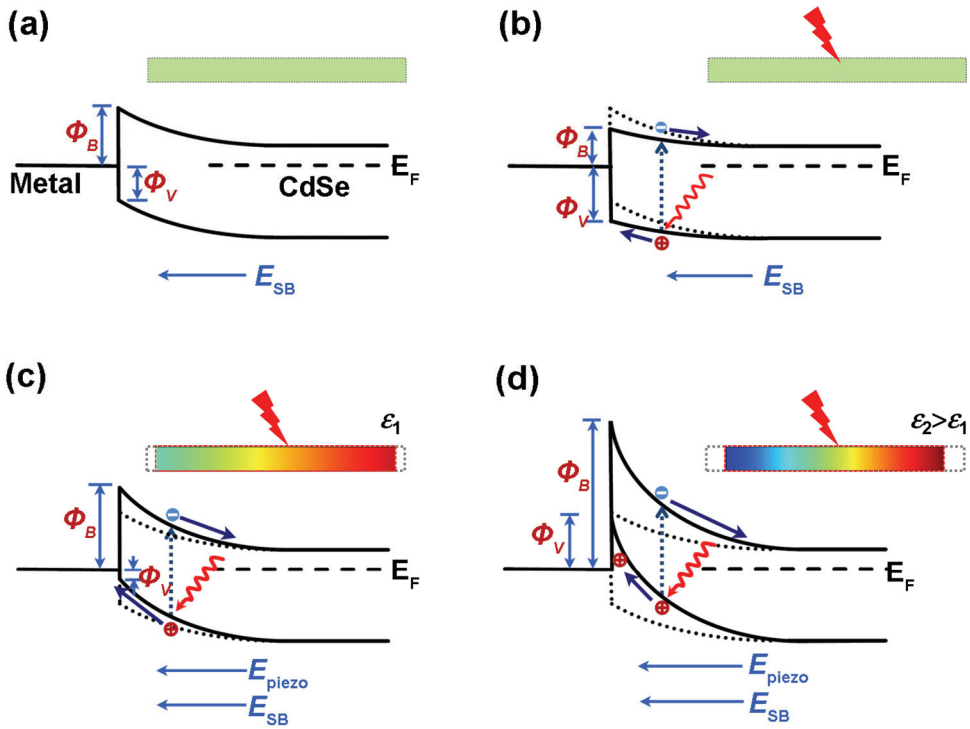

Figure 4. Schematic Energy band diagram for illustrating the piezo-phototronic effect on a Schottky contacted metal-semiconductor interface when (a) neither strain nor illumination, (b) only illumination, (c) slight compressive strain and illumination, (d) large compressive strain and illumination is applied to the CdSe NW device.

the valence band of the CdSe. Hence, the strain required for the optimum sensitivity shifts to higher value when the excitation intensity increases, as shown in Figure 3(c–e).

In summary, the piezo-phototronic effect on transport properties of flexible CdSe NW devices is investigated. The devices exhibit a fast response and recovery on both photo illumination and applied strain. Except for those under low illumination intensity, where the photo-excited electron-hole pairs in the depletion zone are completely separated, the photocurrent rises when the compressive strain is applied, and then decreases after a critical strain is reached. An optimum sensitivity of the flexible CdSe NW devices can be achieved by adjusting the applied strain and illumination intensity. A theoretical model is proposed to explain such effect on the electrical characterization. The piezo-phototronic effect under compressive strain increases the internal electric field of the Schottky barrier, and assists the separation of the photo-excited electron-hole pairs, resulting in the increase of photocurrent. A trap-mediated mechanism is responsible for the decreased hole separation when the strain is over the critical strain. The distinct piezo-phototronic properties of the flexible CdSe NW devices provide us with a versatile potential pathway to tune/control the performance of NW derived opto-electronic devices with coupling photo-excitation and piezo-electric effects.

Materials and Experimental Section

CdSe NWs synthesis and characterization: CdSe NWs were fabricated via the Au-catalyzed vapor–liquid–solid growth process. CdSe powder was placed in the center of the tube furnace, while silicon wafer with 2 nm Au layer was placed 25 cm to the center downstream. The typical synthesis was carried out at the temperature of 820 °C and pressure of 255 Torr for 3 h. Then the CdSe NWs were characterized by SEM (LEO FESEM 1550), TEM with SAD (JEOL-JEM 4000). X-ray diffraction (XRD) measurements were performed on an X'Pert Pro Powder diffractometer from PANalytical (Cu Kα radiation, 40 kV, 40 mA).

Device fabrication: The CdSe NW device was fabricated by transferring an individual CdSe NW laterally onto the polystyrene (PS) substrate, with its *c*-axis in the plane of the substrate. Then we applied silver paste to fix the two ends of the NWs at the substrate, serving as the two electrodes. Finally, a thin layer of polydimethylsiloxane (PDMS) was used to package the device. This PDMS thin layer can prevent the CdSe NWs from contamination or corrosion by gases or liquid. And because of its transparency, it will have little effect on the photodetect process of these devices.

Piezo-phototronic effect on CdSe NWs device: The two ends of the device were separately fixed tightly on the sample holders. Both sample holders are fixed tightly on two three-dimensional mechanical stages to bend the device. We use a solar simulator to provide parallel and uniform intensity light source. To adjust the light intensity, some neutral density filters are utilized. The illumination intensity is calibrated by an optical power meter (Newport, 1916-C). The performances of the device under different strains and different light intensity were measured by a computer-controlled measurement system.

Acknowledgements

This research was supported by NSF (CMMI 0403671), BES DOE (DE-FG02-07ER46394) and the Knowledge Innovation Program of the Chinese Academy of Science (Grant No. KJCX2-YW-M13). L. D. is grateful for the partial support from the National Natural Science Foundation of

China (No. 50902125), China Postdoctoral Foundation (No. 201104371) and Chinese Scholarship Council.

Received: April 5, 2012
Revised: June 25, 2012
Published online:

[1] J. Debaets, J. Vanfleteren, I. Derycke, J. Doutreloigne, A. Vancalster, P. Devisschere, *IEEE. Trans. Electron. Dev* **1990**, *37*, 636.
[2] M. Achermann, M. A. Petruska, S. Kos, D. L. Smith, D. D. Koleske, V. I. Klimov, *Nature* **2004**, *429*, 642.
[3] I. Gur, N. A. Fromer, M. L. Geier, A. P. Alivisatos, *Science* **2005**, *310*, 462.
[4] T. Uematsu, J. Kimura, Y. Yamaguchi, *Nanotechnology* **2004**, *15*, 822; J. Kimura, S. Maenosono, Y. Yamaguchi, *Nanotechnology* **2003**, *14*, 69.
[5] X. J. Ji, J. Y. Zheng, J. M. Xu, V. K. Rastogi, T. C. Cheng, J. J. DeFrank, R. M. Leblanc, *J. Phys. Chem. B* **2005**, *109*, 3793.
[6] Y. Xing, Q. Chaudry, C. Shen, K. Y. Kong, H. E. Zhau, L. WChung, J. A. Petros, R. M. O'Regan, M. V. Yezhelyev, J. W. Simons, M. D. Wang, S. Nie, *Nat. Protoc* **2007**, *2*, 1152.
[7] Q. Yang, X. Guo, W. H. Wang, Y. Zhang, S. Xu, D. H. Lien, Z. L. Wang, *ACS Nano* **2010**, *4*, 6285.
[8] Y. F. Hu, Y. Zhang, Y. L. Chang, R. L. Snyder, Z. L. Wang, *ACS Nano* **2010**, *4*, 4220.
[9] Y. Yang, W. X. Guo, Y. Zhang, Y. Ding, X. Wang, Z. L. Wang, *Nano Lett.* **2011**, *11*, 4812.
[10] Z. L. Wang, *Adv. Mater.* **2007**, *19*, 889.
[11] Q. Yang, W. H. Wang, S. Xu, Z. L. Wang, *Nano Lett.* **2011**, *11*, 4012.
[12] Y. Zhang, G. Gao, H. L. W. Chan, J. Dai, Y. Wang, J. Hao, *Adv. Mater.* **2012**, *24*, 1729; Y. Hu, Y. Zhang, L. Lin, Y. Ding, G. Zhu, Z. L. Wang, *Nano Lett.* **2012**, *12*, 3851,
[13] Z. L. Wang, J. H. Song, *Science* **2006**, *312*, 242; X. D. Wang, J. H. Song, J. Liu, Z. L. Wang, *Science* **2007**, *316*, 102; G. A. Zhu, R. S. Yang, S. H. Wang, Z. L. Wang, *Nano Lett.* **2010**, *10*, 3151.
[14] C. F. Pan, Z. T. Li, W. X. Guo, J. Zhu, Z. L. Wang, *Angew. Chem. Int. Edit.* **2011**, *50*, 11192; C. Xu, Z. L. Wang, *Adv. Mater.* **2011**, *23*, 873.
[15] X. D. Wang, J. Zhou, J. H. Song, J. Liu, N. S. Xu, Z. L. Wang, *Nano Lett.* **2006**, *6*, 2768.
[16] J. H. He, C. L. Hsin, J. Liu, L. J. Chen, Z. L. Wang, *Adv. Mater.* **2007**, *19*, 781.
[17] Y. F. Hu, Y. L. Chang, P. Fei, R. L. Snyder, Z. L. Wang, *ACS Nano* **2010**, *4*, 1234.
[18] Y. Zhang, Y. Yang, Z. L. Wang, *Energy Environ. Sci.* **2012**,*5*, 6850.
[19] S. M. Sze, K. K. Ng, *Physics of Semiconductor Devices, 3rd Edition*, John Wiley & Sons, Inc., Hoboken, New Jersey **2007**.

DOI: 10.1002/adma.201201385